J Mater Sci (2011) 46:4053–4057
DOI 10.1007/s10853-011-5334-x

Effects of addition of potassium chloride and ethylene glycol on nanofluidic behaviors

Weiyi Lu · Taewan Kim · Venkata K. Punyamurtula · Aijie Han · Yu Qiao

Received: 7 December 2010 / Accepted: 25 January 2011 / Published online: 10 February 2011

Abstract Infiltration and defiltration behaviors of liquids modified by potassium chloride and ethylene glycol in a nanoporous silica are investigated through a high-pressure experiment. At the first loading, infiltration can always take place quite smoothly no matter how viscous the liquid is. The infiltration pressure can be well described by linear superposition of the contributions of liquid components. At the second loading, however, only the potassium chloride modified system exhibits a considerable compressibility, suggesting that the effects of the two admixtures on defiltration are different. The irreversibility of the liquid motion may be attributed to the unique liquid structures in nanoenvironment.

Introduction

For a couple of decades, understanding molecular behaviors in nanoenvrionment has been increasingly critical in a large number of areas [e.g., 1–4]. One example is the nanoporous materials functionalized (NMF) liquid, which has great potential for energy absorption and damping [5–7].

W. Lu · V. K. Punyamurtula · Y. Qiao
Department of Structural Engineering, University of California—San Diego, La Jolla, CA 92093-0085, USA

T. Kim · Y. Qiao (✉)
Program of Materials Science & Engineering, University of California—San Diego, La Jolla, CA 92093, USA
e-mail: yqiao@ucsd.edu

A. Han
Department of Chemistry, University of Texas—Pan American, Edinburg, TX 78539, USA

Over many years, "soft" materials, e.g., polymer/metallic foams, were widely utilized in protection devices, such as bumpers and damping tables [8]. Usually, in engineering practice the stiffness of a protection component cannot be too small, which is contradictory to the requirement of high energy absorption and/or wave redistribution capacity. Inspired by the fact that fluids are more "flexible" than solids, people developed liquid/air embedded systems. The successful examples include air beds, air bags, water mattresses, air-venting sport shoes, as well as liquid dampers [e.g., 9–11]. However, different from a soft solid which is of a small bulk modulus, the liquids used in these systems are nearly impressible [12]. Their bulk moduli are typically at the level of 10^9–10^{10} Pa [13], higher than that of foams by a few orders of magnitude. When a stress wave propagates in the liquid phase, the energy that it carries can only be redistributed but not dissipated.

A liquid is of a low shear resistance under ambient condition. Under a dynamic loading where the flowability is partly lost, it can be quite "rigid", sometimes having an amplification effect on impact damage. For instance, it is well known that a polyisoprene layer, which becomes liquid-like when the pressure is high and the time scale is short, can homogenize an intense stress wave, behaving as a wave transfer medium [14].

Modifying a liquid phase by nanoporous materials promises to provide a powerful solution for the above problem [15, 16]. A NMF liquid is usually formed by dispersing nanoporous particles in a liquid. The inner surfaces of nanopores should be lyophobic, so that under ambient pressure they cannot be soaked up spontaneously. Thus, the system becomes a "liquid foam", with nanometer (nm) scale gas phases stabilized by the porous framework. When a sufficiently high pressure is applied

and the capillary effect is overcome, the liquid phase can be forced into the nanopores. Different from the cell buckling in a solid foam, the energy absorption mechanism of a NMF liquid is associated with the increase in interface energy: $\Delta\gamma \cdot A$, where $\Delta\gamma$ is the effective excess interfacial tension and A is the specific surface area. For a solid–liquid system, $\Delta\gamma$ is usually at the level of 10^{-2} J/m^2 [17]; and A of a nanoporous material is typically 10^2–10^3 m^2/g, leading to a high energy absorption efficiency of 1–10 J/g. Its liquid nature assures that the external pressure can be relatively evenly dispersed, so that the shear localization can be reduced and the nanopore surface area can be efficiently utilized. Due to the small length scale, the energy absorption can be completed in only 10^{-7}–10^{-6} s [18, 19], attractive for mitigation of blast wave fronts. Additionally, the "energy capture" effect, i.e., the removal of the energy-carrying liquid medium from the wave transmission path, can further enhance the energy absorption performance.

One important issue that must be solved before the NMF liquids can be widely applied is that it should be functional even in harsh environments. For instance, the military protective devices often demand an operation temperature range of about −20 to 60 °C [e.g., 20]. While the high temperature range is less a problem for an aqueous solution, antifreezing agents need to be used to prevent solidification in the low-temperature range. As the liquid phase is modified, its infiltration and defiltration behaviors may be different. Previously, it has been shown that with a small amount of chemical admixtures, the properties of confined liquids can be significantly varied [21–25].

Experimental

In the current study, a Sigma-Aldrich silica gel was investigated. The as-received materials were in powder form, with the particle size of 10–50 μm. It was first combusted in air at 600 °C for 2 h and repeatedly rinsed in acetone and warm water, followed by vacuum drying at 150 °C for 12 h. About 1 g of the silica gel was mixed with 40 mL of dry toluene in a round bottom flask. After stirring for 5 min, 1.0 mL of chlorotrimethylsilane was injected into the flask, and the mixture was stirred at 90 °C for 48 h. The material was carefully filtered out, rinsed by dry toluene and warm water, and vacuum dried at 80 °C for 12 h. Its nanoporous structure was characterized in a Micromeritics ASAP2000 Gas Absorption Analyzer. The average pore size was measured to be 7.6 nm, in the mesoporous range [26], and the specific nanopore volume was 550 mm^3/g.

A set of NMF liquids were produced by suspending 0.2 g of the treated nanoporous silica gel in 5 g of liquid. The liquid phase was either a saturated potassium chloride (KCl) solution, or ethylene glycol (EG), or a mixture of them. The behaviors of pure water-based system, which will be used as the reference system in the following discussion, have been analyzed elsewhere [27]. Due to the low freezing points of their aqueous solutions, chloride salts and EG are commonly used antifreezes. The molecular formula of EG is $C_2H_4(OH)_2$, of a polar structure with two hydroxyl groups. It is a viscous liquid, with the viscosity of 16.1 mPa s.

The energy absorption experiment was performed by sealing the NMF liquid in a stainless steel cylinder. A steel piston, equipped with a sealing o-ring, was driven into the cylinder by a type 5580 Instron machine at a constant rate of 1 mm/min. The diameter of the piston was 19.0 mm. The pressure was increased to about 40 MPa and then reduced to 0. Similar loading–unloading cycles were repeated for 4–5 times for each sample. In the range of pressure under investigation, the porous structure of the silica gel did not vary [28]. Because for every sample after the second loading the system behavior converged in all the subsequent cycles, only the first two loadings will be analyzed. Figures 1, 2, and 3 show typical sorption isotherm curves of the pressure–volume relationship, demonstrating that the system volume decreases with the increase in applied pressure, and when the pressure is reduced the system volume may partly recover. The curves have been shifted along the horizontal axis to remove the free traveling section of the piston, so that the onset of the pressure rise starts from the origin.

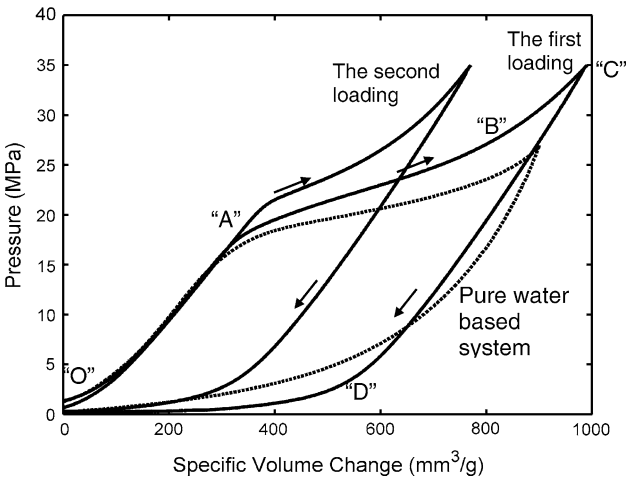

Fig. 1 Typical sorption isotherm curves of the potassium chloride modified system. The *dashed line* indicates the behavior of the pure water based system. The *curves* have been shifted along the horizontal axis

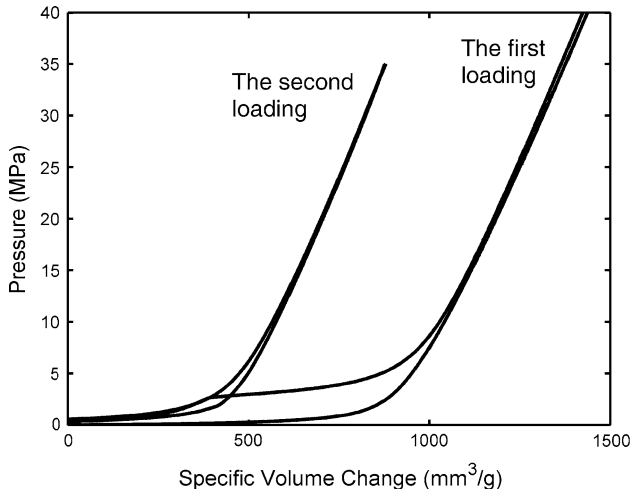

Fig. 2 Typical sorption isotherm curves of the ethylene glycol modified system. The *curves* have been shifted along the horizontal axis

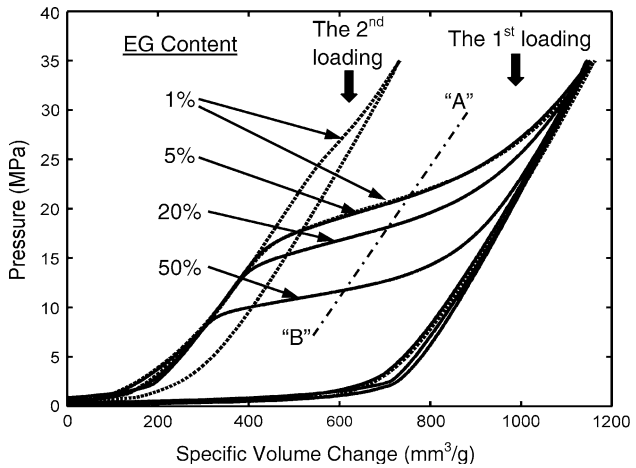

Fig. 3 Typical sorption isotherm curves of the systems modified by both potassium chloride and ethylene glycol. The *curves* have been shifted along the horizontal axis

Results and discussion

During the surface treatment process, chlorotrimethylsilane molecules react with the hydroxyl sites at the silica inner surfaces and form a monolayer of silyl groups. As the polar hydroxyl sites are deactivated by the nonpolar surface groups, the nanopore walls become hydrophobic. From Fig. 1, it can be seen that, compared with the pure water based reference system [27], the addition of KCl does not cause significant changes in the profile of sorption isotherm curve. In the low pressure range ("OA"), no infiltration can be detected. When the pressure is relatively high and the liquid starts to enter the nanopores, the system volume decreases rapidly, leading to the formation of an infiltration plateau ("AB"). When the nanopores are filled, the infiltration plateau ends. The width of the infiltration plateau is close to the measured porosity, as it should be. Upon unloading, the liquid does not defiltrate until the pressure is much lower than the infiltration pressure (P_{in}), after which a defiltration plateau ("DO") is formed. One major change caused by KCl is the variation in P_{in}, which is slightly higher than that of the pure water based system [27]. Clearly, as KCl dissolves in water, the ions can enter the nanopores quite smoothly with the aid of the external pressure. The increase in P_{in} is probably associated with the increase in surface tension of the electrolyte solution [29].

Because in the experiment at the end of each loading–unloading cycle the piston is always forced to return to the original position, the defiltration plateau only partly reflects the liquid defiltration behaviors. The volume of the defiltrated liquid should be estimated by the infiltration plateau width at the second loading. That is, as the loading–unloading cycle is repeated, only the pores that are emptied during the unloading process in the first cycle can be filled again. According to Fig. 1, about 50% of confined liquid defiltrates at the first unloading. The liquid motion in these pores is reversible, and, thus, from the third loading all the subsequent cycles are nearly the same with the second loop. In the rest of the nanopores, the confined liquid does not come out even when the pressure is removed. The hysteresis of the sorption isotherm curves may be related to the difficulty in the formation of vapor phase, which must fill the empty nanopores to maintain the thermodynamic equilibrium [30, 31]; and/or caused by the "column resistance" to the liquid molecules sliding along the solid wall [32]. Recent experiments indicate that liquid defiltration is an endothermic process [33, 34], because of the local entropy change.

If the liquid phase is EG, as shown in Fig. 2, in the first loading–unloading cycle the characteristics of the sorption isotherm curve are similar, except that P_{in} is reduced to about 4 MPa, which may be associated with the low surface tension of EG. Even with the high viscosity, the EG molecules can enter all the nanopores, since the width of the infiltration plateau is nearly the same with that of Fig. 1. In a nanopore, the ordinary boundary layer structure breaks down [35]. At such a small length scale no regular viscosity can be defined, as the relatively motion of liquid molecules cannot be fully developed. As a result, the effective viscosity is considerably reduced [36], so that the internal friction effect becomes secondary.

However, as the second loading is applied, no infiltration can be detected. That is, little confined EG molecules can defiltrate from the nanopores, which may be caused by the difficulty in vapor phase nucleation and growth, the reduced defiltration driving force (P_{in}), the increase in

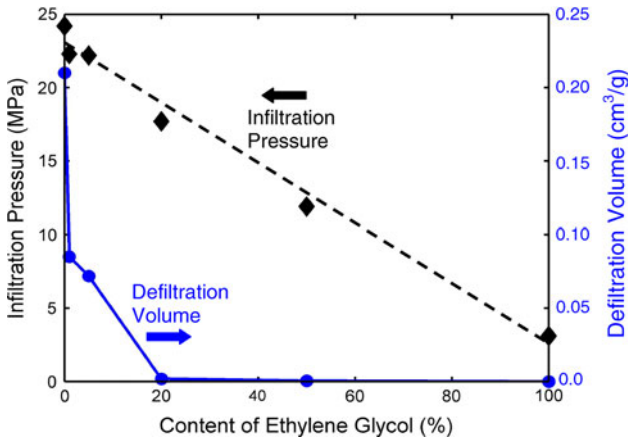

Fig. 4 The infiltration pressure and the defiltration volume as functions of the liquid composition

internal friction, which is trivial under the high infiltration pressure but can be critical in defiltration, as well as the combination of these factors.

Figure 3 indicates that if the liquid phase is a mixture of EG and KCl solution, at the first loading the infiltration can take place upon the application of external pressure. The infiltration volume does not vary with the content of EG (C_{EG}), suggesting that the nanopore surfaces are accessible in all the cases. The value of P_{in} decreases with the increasing of C_{EG}. As shown in Fig. 4, the P_{in}–C_{EG} relationship is quite linear. In this paper, for the purpose of self-comparison, P_{in} is taken as the pressure at the middle point of the infiltration plateau. The middle point is obtained as the intersection of the sorption isotherm curve and the median line of the low-pressure linear compression path and the unloading path (line "AB" in Fig. 3). Clearly, the infiltration behaviors of the liquid mixtures can be dealt with by the linear superposition principle. The interactions between EG molecules, water molecules, and solvated ions do not have a pronounced influence on the effective solid–liquid interfacial tension, which is essentially the area average of the contributions from the liquid components.

The defiltration behaviors, however, are highly nonlinear with respect to C_{EG}. As shown in Figs. 3 and 4, with only 1% of EG, the infiltration plateau width at the second loading is reduced by almost two third. When C_{EG} reaches 5%, the defiltration volume vanishes. These results suggest that the defiltration is governed by the "weakest link". Since the driving force of EG is much lower than that of water and solvated ions, as the external pressure is lowered the EG molecules tend to stay in the nanopores, which can either block the nanopores or drag the water molecules and ions behind. It may also be related to the decrease in effective vapor pressure. As the continuum theory may still work in nanopores as small as a few nm [37], the irreversibility of the confined liquid motion should be related to the surface effects.

Concluding remarks

In summary, through a pressure induced infiltration experiment, it is validated that infiltration can occur smoothly in NMF liquids modified by potassium chloride and ethylene glycol. Upon the removal of external pressure, about 50% of confined liquid can defiltrate in the KCl modified system, while the defiltration in EG modified system is negligible. When KCl solution and EG are mixed together, the infiltration behaviors can be regarded as the linear superposition of the contributions of the two components, but the defiltration behaviors are highly nonlinear. The irreversibility of the motion of complex liquid in nanopores suggests that the continuum theory breaks down at such a small length scale. The details of the interactions among the solid atoms and the confined liquid phase are still quite inadequately understood.

Acknowledgements This work was supported by the National Science Foundation under Grant No. ECCS-1028010.

References

1. Nattua D, Gogotsi Y (2008) Microfluid Nanofluid 5:289
2. Matos J, Garcia A, Poon PS (2010) J Mater Sci 45:4934. doi: 10.1007/s10853-009-4184-2
3. Chadwick EG, Clarkin OM, Tanner DA (2010) J Mater Sci 45:6562. doi:10.1007/s10853-010-4745-4
4. Mirzaeian M, Hall PJ (2009) J Mater Sci 44:2705. doi: 10.1007/s10853-009-3355-5
5. Surani FB, Kong X, Panchal DB, Qiao Y (2005) Appl Phys Lett 87:163111.1-3
6. Han A, Qiao Y (2006) J Am Chem Soc 128:10348
7. Surani FB, Han A, Qiao Y (2006) Appl Phys Lett 89:093108.1-3
8. Lu G, Yu T (2003) Energy absorption of structures and materials. CRC Press, Baton Raton, FL
9. Kent RW (2003) Air bag development and performance. Society of Automotive Engineers, Warrendale, PA
10. Villaverde R (2009) Fundamental concepts of earthquake engineering. CRC Press, Baton Raton, FL
11. Cheskin MP (1987) The complete handbook of athletic footwear. Fairchild Books, New York
12. Cengel Y, Cimbala J (2009) Fluid mechanics. McGraw-Hill, New York
13. Poling BE, Prausnitz JM, O'Connell JP (2003) The properties of gases and liquids. McGraw-Hill, New York
14. Brebbia CA, Nurick GN (2003) Advances in dynamics and impact mechanics. WIT Press, Southampton

15. Chen X, Surani FB, Kong X, Punyamurtula VK, Qiao Y (2006) Appl Phys Lett 89:241918.1-3
16. Surani FB, Qiao Y (2006) J Appl Phys 100:034311.1-4
17. Ibach H (2006) Physics of surfaces and interfaces. Springer, Berlin
18. Chen X, Cao G, Han A, Punyamurtula VK, Liu L, Culligan PJ, Kim T, Qiao Y (2008) Nano Lett 8:2988
19. Qiao Y, Liu L, Chen X (2009) Nano Lett 9:984
20. Military Standard (1985) Polymer matrix composites. MIL-STD-1944, June 10th
21. Kim T, Lu W, Han A, Punyamurtula VK, Chen X, Qiao Y (2009) Appl Phys Lett 94:013105.1-3
22. Lu W, Han A, Kim T, Punyamurtula VK, Chen X, Qiao Y (2009) Appl Phys Lett 94:023106.1-3
23. Kong X, Surani FB, Qiao Y (2006) Phys Scr 74:531
24. Kong X, Surani FB, Qiao Y (2005) J Mater Res 20:1042
25. Cao GX, Qiao Y, Zhou QL, Chen X (2008) Mol Simul 34:1267
26. Polarz S, Smarsly B (2002) J Nanosci Nanotechnol 2:581
27. Kong X, Qiao Y (2005) Appl Phys Lett 86:151919.1-3
28. Han A, Punyamurtula VK, Lu W, Qiao Y (2008) J Appl Phys 103:084318.1-5
29. Bockris JOM, Khan SUM (2003) Surface electrochemistry: a molecular level approach. Springer, New York
30. Han A, Kong X, Qiao Y (2006) J Appl Phys 100:014308.1-3
31. Qiao Y, Cao G, Chen X (2007) J Am Chem Soc 129:2355
32. Zhao J, Culligan PJ, Qiao Y, Zhou Q, Li Y, Tak M, Park T, Chen X (2010) J Phys: Condens Matter 22:315301.1-12
33. Han A, Lu W, Punyamurtula VK, Kim T, Qiao Y (2009) J Appl Phys 105:024309.1-4
34. Han A, Punyamurtula VK, Qiao Y (2008) J Mater Res 23:1902
35. Liu L, Qiao Y, Chen X (2008) Appl Phys Lett 92:101927.1-3
36. Han A, Lu W, Punyamurtula VK, Chen X, Surani FB, Kim T, Qiao Y (2008) J Appl Phys 104:124908.1-4
37. Bocquet L, Charlaix E (2010) Chem Soc Rev 39:1073